Comparison and combined use of two sand constitutive models

G. VANNUCCHI *

SUMMARY: Many studies have been and are being carried out on the stress-strain relationships in cohesionless soils. These studies have produced various constitutive models: among these, the elastic non linear hyperbolic model [KONDNER, 1963; DUNCAN and CHANG, 1970] and the elasto-plastic model with curved yield surface [LADE, 1977].

These two models, although so different in concept, can, however, be considered in part complementary. In the first, a simple constitutive equation permits the representation of the experimental total stress-strain diagram for drained triaxial tests in a range of deviatoric stresses between 70 and 95% of failure. The second model, which analyses the components of elastic and plastic strains in detail, is capable of describing complex load processes even after failure by using an incremental analysis.

The parameters which must be evaluated for the application of Lade's model are subject to gross errors which it is hard to check. This comes about because they result from a complex numerical processing of experimental data of different levels of accuracy.

It's possible to get over such difficulty utilizing as input data not experimental values, directly measured, but values from a simple elastic non linear stress-total strain relationship (filter model).

Thus the hyperbolic model is used in this paper as a filter for the experimental data to which Lade's elasto-plastic model will be applied. The criterion followed consists in making a comparison between two constitutive models of different types and with different characteristics, and examining the theoretical consequences which arise from having filtered the experimental data with one model before processing and using them for the calculation of the coefficients of the other. The result of such an operation is a serie of equations which permit the theoretical calculation of the components of strain and of the parameters ν_p, η, (W_p/p_a).

The calculated values that fall within the filter model's most reliable range, agree very closely with the direct experimental values and also with the empirical relations proposed by Lade.

In the range in which the filter model is less representative, where a direct comparison is possible (ε_{ij}, W_p/p_a) there is agreement between experimental and theoretical values; where, on the contrary, a direct comparison is impossible because of the lack of reliable experimental values (ν_p, η_2), asymptotic patterns are attained which, although cannot be exluded a priori, require deeper critical attention.

1. Introduction

The last few years have seen an increase in the study of the constitutive laws of soil which has been made possible by the rapid advance of technological progress. Sophisticated laboratory equipment such as the cubic triaxial instrument has permitted the analysis of the behaviour of soils subjected to any possible succession of stresses and strains. Meanwhile, the development of numerical analysis techniques has meant the practical utilization of the knowledge gained in the laboratory in geotechnical design.

Although it is certainly good that better equipped research centres should be able to carry out complex experimental programmes addressed to the definition of various aspetcs of the geotechnical behaviour of soils, a synthetic view of the knowledge acquired is also necessary in order to indicate whether and how it is possible to obtain useful results also in laboratories which have standard equipment only. P. V. Lade's work is particularly useful in this respect. Having studied the behaviour of cohesionless soils by means of the cubic triaxial equipment [LADE and DUNCAN, 1973], he produced an elasto-plastic theory in which the parameters of the calculation are determined exclusively by means of standard triaxial tests [LADE, 1977].

Stress-strain relationships of cohesionless soils are influenced by a large number of factors such as, for example, the geometry and density of the solid structure, the water content and drainage conditions, the mode of application of loads, the stress history. For these reasons those mathematical models which use experimental parameters that are easily determined and which, at the same time, describe at least the most important aspects of the behaviour with sufficient accuracy, must be preferred.

Among the continuous models for cohesionless soils, the hyperbolic non-linear model [KONDNER, 1963; DUNCAN and CHANG, 1970] and the elasto-plastic model with curved yield surfaces [LADE, 1977] are of particular interest both because of the numerical applications to which they have given rise, and because they

* Dott. Ing. Giovanni Vannucchi, Dipartimento di Ingegneria Civile, Università di Firenze.

can be quantitatively defined on the basis of standard laboratory tests. The first model permit the description of the total stress-strain curve almost to the point of failure by means of few, easily determined parameters which have immediate physical significance. It has been successfully used in problems of geotechnical design and verification tackled by finite element [CHANG and DUNCAN, 1970; KULHAWY and DUNCAN, 1972]. The second model, which analyses the components of elastic and plastic strain in detail, is capable of describing complex load processes even after the point of failure has been reached by using an incremental type of analysis.

These two models, although different in concept, are not incompatible and can be considered in part as complementary. Lade's model, which is more detailed and exhaustive from the theoretical point of view, requires a quantity of numerical calculations based on the results of standard triaxial and hydrostatic compression tests. It is well known that experimental data, even if obtained in a formally correct manner from repeated tests, always contain a certain degree of uncertainty. This is due both to the inevitable differences in the geometrical and geotechnical characteristics of different samples and to the limited sensitivity of the measuring instruments and the accidental errors introduced by the researcher in the various stages of testing. If, then, the parameters to be evaluated is not directly measured but is the result of a numerical processing of experimental data of differing degrees of accuracy (and especially if it is the result of a difference between high value quantities), a formally more correct parameter can be less reliable numerically.

Every geotechnical researcher knows at least the magnitude of the quantity which he is measuring and thus, on the basis of his experience, is able to carry out a critical rule of thumb evaluation of the results obtained. However when the quantities calculated do not have immediate physical signifiance, such a critical evaluation becomes much more difficult.

It is for these reasons that it has been considered useful to filter the experimental values through Kondner's hyperbolic model and apply Lade's elasto-plastic model to the normalized total stress-strain diagram thus obtained. This has been made possible by making a few marginal modifications to the hyperbolic model (in particular with regard to the failure criterion), determining an experimental relationship between volumetric stresses and strains, and above all omitting the description of the softening behaviour of dense sands.

Kondner's model reproduces well the experimental stress-strain diagram for stresses between 70% and 90% of the value at the point of failure [DUNCAN and CHANG, 1970]. In this range it can thus be used as a non deforming filter for experimental data. For a complete exposition of the theoretical premises and of the notation, the reader is referred to the original papers [DUNCAN and CHANG, 1970; LADE, 1977].

2. Experimental integrative relations

During a drained triaxial test it is possible to evaluate the volumetric strain of a sample by measuring the quantity of water expelled or absorbed. The experimental curve for dense sand obtained in this way is quantitatively indicated in Fig. 1a. Taking curve $(\varepsilon_v + \varepsilon_1)/\varepsilon_1$ as ordinates and $(\varepsilon_v + \varepsilon_1)$ as abscissas, this curve becomes the curve in Fig. 1b, which can be conveniently approximated by the bilateral 1-2-3. The 1-2 portion preceeds failure and has the equation:

$$(\varepsilon_v + \varepsilon_1)/\varepsilon_1 = - A\,(\varepsilon_v + \varepsilon_1) + B \qquad (1)$$

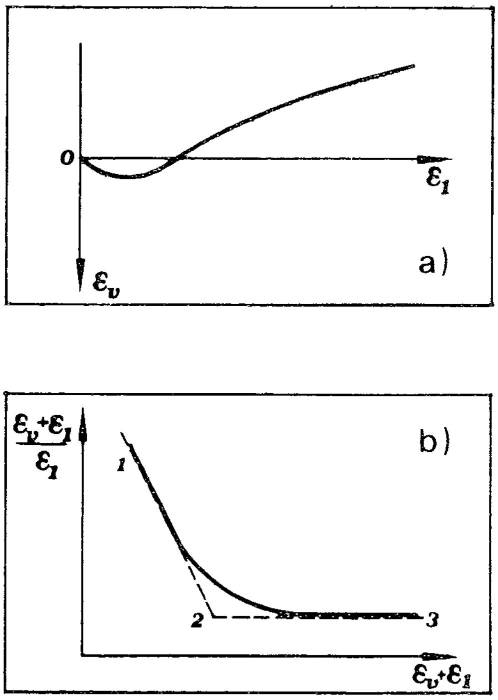

Fig. 1. - Axial and volumetric strains (total) of a sample of dense saturated sand in a drained compression traxial test.
Fig. 1. - Deformazioni assiali e volumetriche totali di un campione di sabbia densa satura in prova triassiale drenata.

The line 2-3 is the horizontal asymptote of the equation:

$$(\varepsilon_v + \varepsilon_l)/\varepsilon_l = D \qquad (2)$$

The intersection 2 of the two strainght lines corresponds to the maximum deviatoric stress during the test (1).

The coefficients A, B, D are experimental functions of the cell pressure. On the basis of equations (1) and (2), the total radial strain before failure is:

$$\varepsilon_3 = \frac{\varepsilon_l\,[0.5\,B - (1 + A\varepsilon_l)]}{(1 + A\varepsilon_l)} \qquad (3)$$

and after failure:

$$\varepsilon_3 = (0.5\,D - 1)\,\varepsilon_l \qquad (4)$$

Poisson's tangent coefficient ν_t is thus, before failure:

$$\nu_t = 1 - \frac{0.5\,B}{(1 + A\varepsilon_l)^2} \qquad (5)$$

and after failure:

$$\nu_t = (1 - 0.5\,D) \qquad (6)$$

The initial (elastic) value is:

$$\nu_i = (1 - 0.5\,B) \qquad (7)$$

The results of an isotropic compression are well represented by the following relation [VANNUCCHI, 1980]:

$$\varepsilon_v = A_1 \left[\frac{\sigma_3}{p_a}\right]^{B_1} \qquad (8)$$

where A_1 and B_1 are two material constants.

Since in this case the plastic expansive strain ε_v^p is zero, the total volumetric strain ε_v is composed by elastic strain ε_v^e and plastic collapse strain ε_v^c:

$$\varepsilon_v = \varepsilon_v^e + \varepsilon_v^c \qquad (9)$$

The elastic component can be calculated by Hooke's law:

$$\varepsilon_v^e = \frac{3}{E}\,\sigma_3\,(1 - 2\nu) \qquad (10)$$

where

$E = E_{ur}$ is unloading-reloading modulus [DUNCAN and CHANG, 1970],

$\nu = \nu_i$ is Poisson's elastic coefficient expressed by (7).

The volumetric plastic collapse strain component can thus be obtained from the difference between (8) and (10):

$$\varepsilon_v^c = \varepsilon_v - \varepsilon_v^e = A_1 \left[\frac{\sigma_3}{p_a}\right]^{B_1} - \frac{3}{E}\,\sigma_3\,(1 - 2\nu) \qquad (11)$$

The plastic work of collapse during an isotropic compression test is obtained from eq (12)

$$dW_c = \left[\frac{\sigma_3}{p_a}\right] d\varepsilon_v^c \qquad (12)$$

whence, taking account of eq (11)

$$\frac{W_c}{p_a} = \left[\frac{\sigma_3}{p_a}\right] d\varepsilon_v^c = \frac{A_1 B_1}{(B_1 + 1)} \left[\frac{\sigma_3}{p_a}\right]^{B_1 + 1} - \frac{3\,(1 - 2\nu)\,(1 - n)}{K\,(2 - n)} \left[\frac{\sigma_3}{p_a}\right]^{2 - n} \qquad (13)$$

or, in function of the degree of hardening $f_c = I_1^2 + 2I_2$

$$\frac{W_c}{p_a} = A_3 \left[\frac{f_c}{p_a^2}\right]^{B_3} - A_4 \left[\frac{f_c}{p_a^2}\right]^{B_4} \qquad (14)$$

where

$$A_3 = \frac{A_1 B_1}{(B_1 + 1)\,3^{0.5\,(B_1 + 1)}}\ ;\ B_3 = 0.5\,(B_1 + 1) \qquad (14a)$$

$$A_4 = \frac{(1 - 2\nu)\,(1 - n)\,3^{0.5n}}{K\,(2 - n)}\ ;\ B_4 = 0.5\,(2 - n) \qquad (14b)$$

are adimensional parameters.

(1) The relations (1) and (2) are derived from those proposed by KULHAWY and DUNCAN [1972], taking into account the convention on signs commonly adopted in geotechnics, i.e. positive sign for compression stresses and shortening strains.

Since it results experimentally that B_3 and B_4 have very similar values while A_3 is significantly larger than A_4, the second term in the r.h.s. of eq (14) can be neglected with respect to the first term: the expression found agrees well with the corresponding law proposed by Lade:

$$\frac{W_c}{p_a} = C\left[\frac{f_c}{p_a^2}\right]^p \tag{15}$$

where it has been put $A_3 = C$ and $B_3 = p$

The criterion of failure [LADE, 1977] (fig. 2)

$$f_p = \left[\frac{I_1^3}{I_3} - 27\right]\left[\frac{I_1}{p_a}\right]^m \tag{16a}$$

$$f_p = \eta_1 \text{ at failure} \tag{16b}$$

takes into account the curvature of the generatrix of the plasticization cone caused by the decrease of the angle of friction as the pressure of containment increases. Such a criterion has been adopted instead of Mohr-Coulomb's for cohesionless soil

$$(\sigma_1 - \sigma_3) = \sin\varphi \cdot (\sigma_1 + \sigma_3) \tag{17}$$

which was used by Duncan and Chang, because it is more general. Experimentally it results that the numerical values of exponent m is close to zero, a value for which the failure surface has rectilinear generatrices and the two criteria cited coincide.

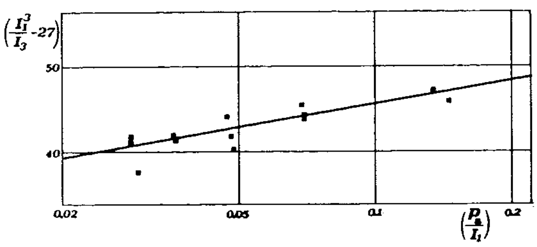

Fig. 2. - Lade's failure criterion.
Fig. 2. - Criterio di rottura di Lade.

3. Calculation of the components of strain

Total axial strains are calculated using the hyperbolic constitutive equation [KONDNER, 1963]:

$$(\sigma_1 - \sigma_3) = \frac{\varepsilon_1}{a + b\varepsilon_1} \tag{18}$$

The coefficient *a* is calculated by means of the expression:

$$\frac{1}{a} = E_{ur} = K_{ur}\, p_a \left[\frac{\sigma_3}{p_a}\right]^n \tag{19}$$

already used [LADE and DUNCAN, 1975] to express the initial tangent modulus.

Coefficient *b*, on the other hand, is derived from LADE'S [1977] criterion of failure on the hypothesis that the failure ratio R_f is a constant of the material:

$$\left\{\frac{\left[\dfrac{R_f}{b} + 3\sigma_3\right]^3}{\sigma_3\left[\left[\dfrac{R_f}{b} + 3\sigma_3\right] - 2\sigma_3\right]^2} - 27\right\} \tag{20}$$

$$\left[\frac{R_f}{p_a b} + 3\left[\frac{\sigma_3}{p_a}\right]\right]^m = \eta_1$$

The strain components are calculated according to the following succession:

— The total volumetric and radial strains before failure are calculated respectively by (1) and (3).

— The elastic strain components are calculated by Hooke's law (eq. 10) using the elasticity modulus defined by (19) and Poisson's coefficient defined by (7).

— The increases in the plastic collapse components during triaxial testing are calculated by the flow rule:

$$\Delta\varepsilon^c_{ij} = \Delta\lambda_c \frac{\partial f_c}{\partial\sigma_{ij}} \tag{21}$$

using the work-hardening law (14).

In standard triaxial compression tests, the derivatives of f_c with respect to the normal stresses are:

$$\frac{\partial f_c}{\partial\sigma_1} = 2\sigma_1 \; ; \; \frac{\partial f_c}{\partial\sigma_3} = 2\sigma_3$$

therefore

$$\Delta\varepsilon^c_1 = 2\sigma_1\,\Delta\lambda_c \tag{21a}$$

$$\Delta\varepsilon^c_3 = 2\sigma_3\,\Delta\lambda_c \tag{21b}$$

The proportionality constant:

$$\Delta\lambda_c = \frac{\Delta W_c}{2 f_c} \qquad (22)$$

is the increment in plastic collapse work over the increment $\Delta f_c > 0$ obtained by differentiation of eq (14). The integration of (21) is carried out numerically.

— Finally, the expansive plastic strain components are calculated by difference:

$$\Delta\varepsilon^p_{ij} = \Delta\varepsilon_{ij} - \Delta\varepsilon^e_{ij} - \Delta\varepsilon^c_{ij} \qquad (23)$$

4. Experimental investigation

The numerical verification of the proposed procedure has been conducted on the basis of the results of 18 triaxial standard drained tests and 2 drained isotropic compression tests. The material used is a uniform fine sand from Torre del Lago Puccini (Lucca). The initial dimensions of the samples, prepared at an initial dry density of 1.75 ± 0.02 were 5.05 cm diameter, 11.10 cm height. Velocity of deformation in the triaxial tests was 0.2 mm/min, consolidation between 40 and 1000 KN/m^2.

Effective stresses were calculated taking into account the axial and volumetric strains of the sample during the test. We believe that the number of tests performed is such to limit the effect of accidental errors and to reduce the influence of individual values on the determination of experimental laws. The latter have, in fact, been determined by excluding, in the calculation of empirical coefficients, those tests which had a result different from the general pattern of the others. Thus the correlation coefficients always resulted larger than 0.90.

5. Analysis of experimental results

For the material described and within the range of pressure considered, coefficient A of eq. (1) is a linearly decreasing function of the cell pressure:

$$A = a_1 \left(\frac{\sigma_3}{p_a} \right) + b_1, \qquad (24)$$

coefficient B is a constant of the material and coefficient D of eq. (2) is a linearly increasing function (Figs. 3a, b, c):

$$D = a_2 \left(\frac{\sigma_3}{p_a} \right) + b_2 \qquad (25)$$

Consequently the Poisson elastic coefficient expressed by eq. (7) is a constant of the material. The numerical values of the constants which have been determined directly are presented in the Appendix .

From the knowledge of the direct experimental constants, it is possible to reconstruct and analyse a drained triaxial test at a constant cell pressure.

As examples, the diagrams relative to two drained triaxial compression tests, in which the cell pressure (σ_3/p_a) was equal to 2 and 5, are presented.

The plots of Fig. 4 refer to the axial strain: the total strain ε_1 is represented by Kondner's hyperbola (eq. 18); the elastic strain component ε_1^e [eqs. (22), (10)] is a straight line; the plastic collapse strain component ε_1^c is obtained incrementally from (21), and the expansive plastic strain component ε_1^p by difference (eq. 23).

The plots of Fig.5 refer to radial strain: ε_3 is obtained by applying (3); the elastic component ε_3^e is a straight line fairly close to the

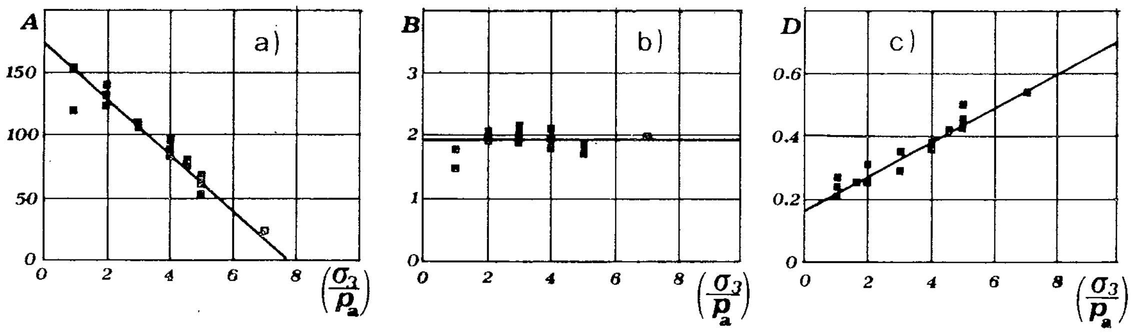

Fig. 3. - Experimental determination of coefficients A, B, D of eqs. (1) and (2) for calculation of total volumetric strains.
Fig. 3. - Determinazione sperimentale dei coefficienti A, B, D delle eqs. (1) e (2) per il calcolo delle deformazioni volumetriche totali.

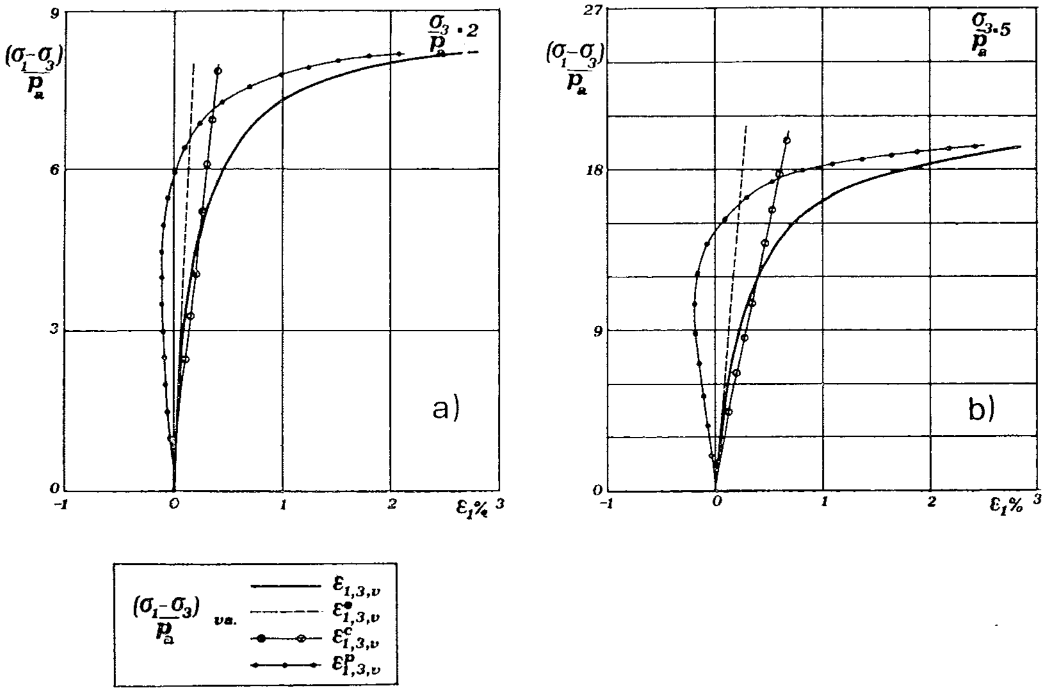

Fig. 4. - Total axial strains and axial strain components in drained triaxial test.

Fig. 4. - Deformazioni assiali totali e componenti di deformazione assiale in prova triassiale drenata.

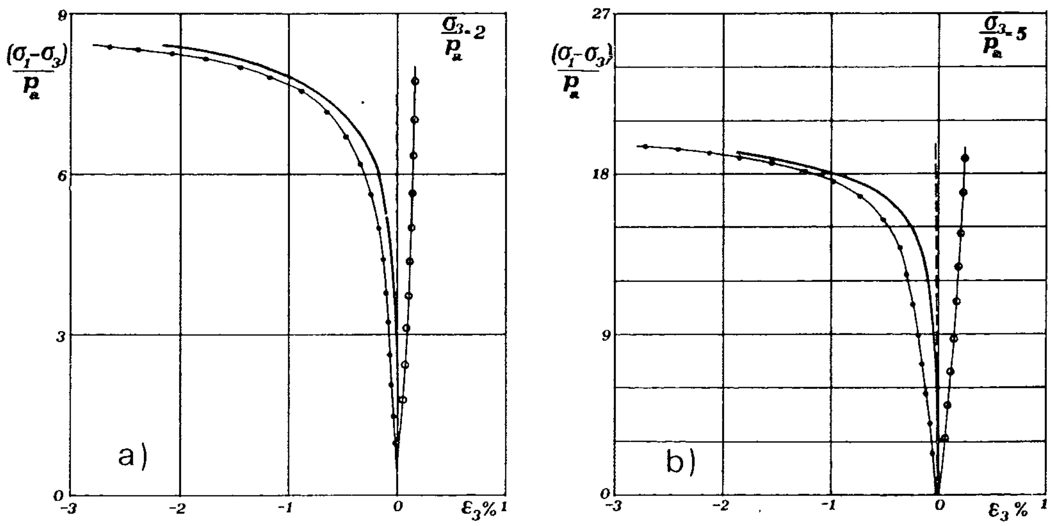

Fig. 5. - Total radial strains and radial strain components in drained triaxial test.

Fig. 5. - Deformazioni radiali totali e componenti di deformazione radiale in prova triassiale drenata.

axis of the ordinate [eqs. (26), (10)]; the plastic collapse strain component ε_3^c is obtained incrementally from eq. 21 and the expansive collapse strain component ε_3^p by difference (eq. 23).

The plots of Fig. 6 refer to volumetric strain: the strain components are obtained by the algebraic sum:

$$\varepsilon_v = \varepsilon_1 + 2\varepsilon_3 \tag{26}$$

Observing the plots of Fig. 4 it can be noted that the axial expansive plastic strain component has at first a negative slope which becomes positive when the deviatoric stress grows. On the contrary, the radial expansive plastic strain component always has negative slope. Thus the coefficient ν_p defined by Lade:

$$\nu_p = -\frac{\Delta\varepsilon_3^p}{\Delta\varepsilon_1^p} \tag{27}$$

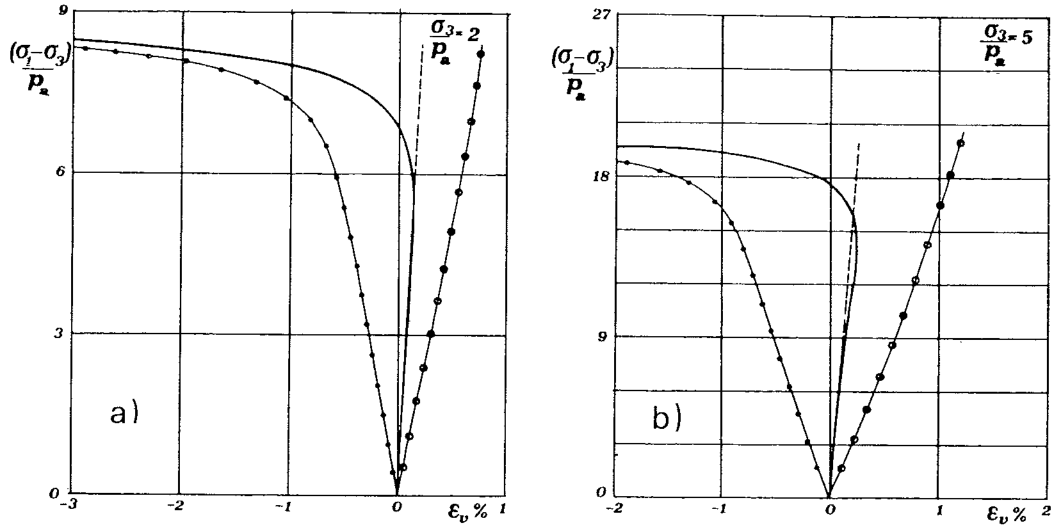

Fig. 6. - Total volumetric strains and volumetric strain components in drained triaxial test.
Fig. 6. - Deformazioni volumetriche totali e componenti di deformazione volumetrica in prova triassiale drenata.

has an horizontal asymptote for that critical deviatoric stress corresponding to the zero value of increment of axial expansive plastic strain (Fig. 7). For deviatoric stress below the critical value, ν_p is negative, while for stress above that value it is positive. In particular, in the range of greatest validity of the filter model — i.e. for stresses between 70% and 95% of the failure value — ν_p has values which are more or less constant at around 0.8 ÷ 1,0, indipendent on cell pressure. It is interesting to note that a determination of ν_p based directly on triaxial tests gave scattered values, for the initial phases of the test and more or less constant ones (0.8 ÷ 1.0) for the phases immediately proceeding failure.

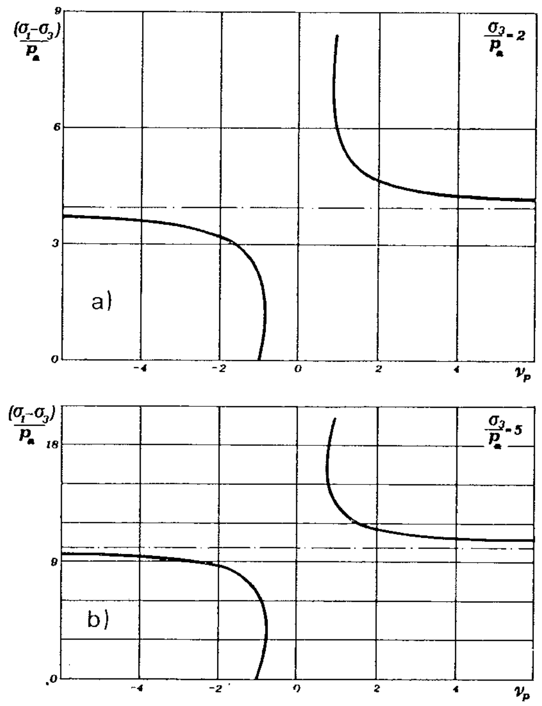

Fig. 7. - Coefficient ν_p vs. $(\sigma_1 - \sigma_3)/p_a$ in drained triaxial test.
Fig. 7. - Variazione del coeff. ν_p con $(\sigma_1 - \sigma_3)/p_a$ in prova triassiale drenata.

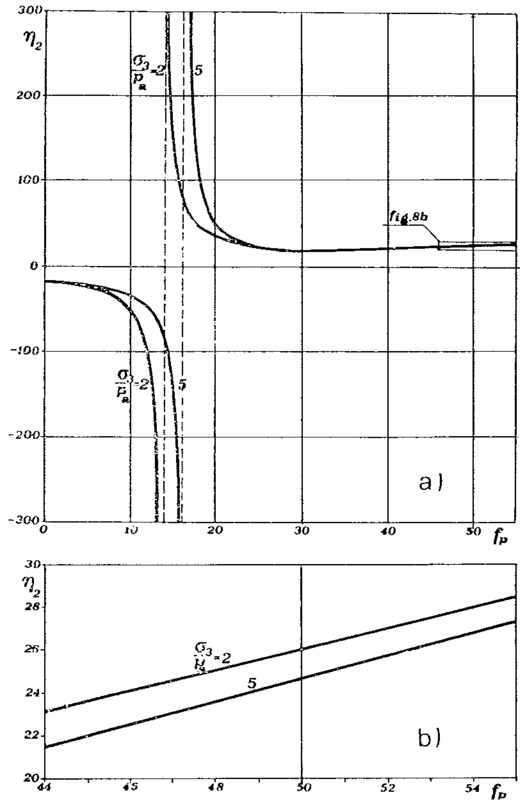

Fig. 8. - η_2 vs. f_p in drained triaxial test.
Fig. 8. - Variazione di η_2 con f_p in prova triassiale drenata.

Fig. 8 is the graphic representation of the equation:

$$\eta_2 = \frac{3\,(1 + \nu_p)\, I_1^2 - 27\,\sigma_3\,(\sigma_1 + \nu_p\,\sigma_3)}{\left(\dfrac{p_a}{I_1}\right)^m \left[\sigma_3\,(\sigma_1 + \nu_p\,\sigma_3) - \dfrac{m\,(1 + \nu_p)\, I_1^2}{f_p \left(\dfrac{p_a}{I_1}\right)^m + 27}\right]} \tag{28}$$

In this case, too, the function shows two distinct branches with a common asymptot at a value of f_p corresponding to the critical deviatoric stress (Fig. 8a). This occurs for reasons analogous to those stated above. The part of the curve corresponding to the range of greater validity of the filter model is more or less rectilinear (Fig. 8b) and agrees excellently with the empirical relation [LADE, 1977]:

$$\eta_2 = Sf_p + R\sqrt{\frac{\sigma_3}{p_a}} + t \tag{29}$$

The relation between total plastic work W_p/p_a and degree of work hardening f_p represented in Fig. 9 is a monotonically increasing positive function which agrees extremely well with the direct experimental results up to very close to the point of failure.

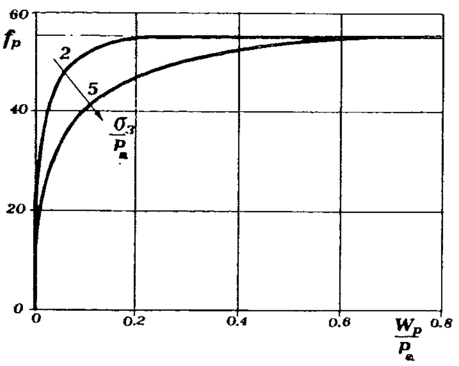

Fig. 9. - Total plastic work W_p/p_a vs. degree of work-hardening f_p in drained triaxial test.

Fig. 9. - Variazione del lavoro plastico totale W_p/p_a in funzione del grado di incrudimento f_p in prova triassiale drenata.

6. Conclusions

A primary purpose of this paper, apart from presenting specific results, is to propose a new method of analysis of the experimental behaviour of materials. The criterion followed in this paper consists in a comparison and combined use of two constitutive models of different types and with different characteristics and in filtering the experimental data through one model before processing and using these data for the calculation of the coefficients of the other model.

In the specific case considered, the experimental stress-strain curve for triaxial tests on sand has a pattern which is slightly different from Kondner's hyperbola in both the low and the high levels of strain [DUNCAN and CHANG, 1970]. In spite of this, in those points where comparison is possible, the numerical results obtained employing the methodology set out above agree extremely well with results obtained from direct experimental methods.

NOTATION

a	: reciprocal of initial tangent modulus and reciprocal of unloading-reloading modulus
a_1, a_2	: direct adimensional experimental constants
A	: volumetric strain parameter in drained triaxial test
A_1	: direct adimensional experimental constant
A_3, A_4	: adimensional experimental constants
b	: reciprocal of asymptotic values of stress difference
b_1, b_2	: direct adimensional experimental constants
B	: volumetric strain parameter in drained triaxial test
B_1	: direct adimensional experimental constant
B_3, B_4	: adimensional experimental constants
C	: collapse modulus
D	: volumetric strain parameter in drained triaxial test
E	: Young's modulus
E_{ur}	: unloading-reloading modulus
f_c	: function describing the spherical yield cap and the degree of hardening
f_p	: function describing failure criterion and failure surface
g_p	: plastic potential function
I_1, I_3	: first and third stress invariants
K_{ur}	: modulus number for unloading-reloading
m	: slope of the straight line in failure criteron

n : exponent

p : collapse exponent

p_a : atmospheric pressure

R : constant

R_f : failure ratio

S : constant

t : constant

W_c : plastic collapse work

W_p : total plastic work

Δ : denote a change in the appended quantity

$\Delta\lambda_p$: proportionality constant enter strain increments and derivatives of the plastic potential

λ_c : proportionality constant

ε_1, ε_3 : principal strains

ε_v : volumetric strain

ε_{ij} : strain tensor

ε^e : elastic strain component

ε^c : plastic collapse strain component

ε^p : plastic expansive strain component

η_1 : value of f_p at failure

η_2 : parameter

ν_t : tangent Poisson's ratio

ν_p : ratio of plastic expansive strain components

σ_1, σ_3 : principal stresses

APPENDIX

EXAMPLE OF CALCULATION: *triaxial test with* $\left(\frac{\sigma_3}{p_a}\right) = 2 = \text{cost}$

For the calculation of:

$a_1 = -22.7$ $b_1 = 172.25$ $B = 1.91 \pm 0.13$ $a_2 = 0.054$ $b_2 = 0.17$	total volumetric and radial strains coefficient of Poisson (Fig. 3)
$K_{ur} = 2654$ $n = 0.602$	elasticity modulus
$R_f = 0.94$	failure ratio
$A_1 = 0.006813$ $B_1 = 0.5616$	total volumetric strains in isotropic compression tests
$\eta_1 = 55.113$ $m = 0.0828$	failure criterion (Fig. 2)

TABLE 1

Direct experimental values measured in triaxial drained compression test with $[\sigma_3/p_a] = 2 = \text{const.}$

Valori sperimentali misurati in prova di compressione triassiale drenata con $[\sigma_3/p_a] = 2 = \text{cost.}$

(1) $\frac{(\sigma_1-\sigma_3)}{p_a}$	(2) $\varepsilon_1\%$	(3) $\varepsilon_v\%$	(4) $\frac{\varepsilon_1\%}{\frac{(\sigma_1-\sigma_a)}{p_a}}$	(5) $(\varepsilon_1+\varepsilon_v)\%$	(6) $\frac{(\varepsilon_1+\varepsilon_v)}{\varepsilon_1}$
0.00	0.00	0.00	—	0.00	—
1.42	0.07	0.07	0.049	0.14	2.00
2.76	0.13	0.10	0.047	0.23	1.77
4.00	0.18	0.12	0.045	0.30	1.67
4.78	0.28	0.15	0.059	0.43	1.54
5.59	0.37	0.15	0.066	0.52	1.41
6.31	0.53	0.10	0.084	0.63	1.19
6.77	0.69	0.02	0.102	0.71	1.03
7.05	0.85	−0.07	0.121	0.78	0.92
7.29	0.99	−0.17	0.136	0.82	0.83
7.47	1.20	−0.27	0.161	0.93	0.78
7.67	1.36	−0.39	0.177	0.97	0.71
7.78	1.54	−0.53	0.198	1.01	0.66
7.91	1.73	−0.68	0.219	1.05	0.61
7.98	1.92	−0.83	0.241	1.09	0.57
8.15	2.13	−0.97	0.216	1.16	0.54
8.24	2.29	−1.07	0.278	1.22	0.53
8.30	2.49	−1.24	0.300	1.25	0.50
8.34	2.69	−1.38	0.322	1.31	0.49
8.36	2.87	−1.53	0.343	1.34	0.47
8.41	3.26	−1.84	0.388	1.42	0.44
8.42	3.44	−1.99	0.409	1.45	0.42

Kondner's hyperbola parameters:

from data of table 1

$a = 0.02918\%$

$b = 0.1094$

$r = 0.9996$ (correlation coeff.)

$E_{ur} = 1/a = 3427$

$\frac{(\sigma_1 - \sigma_3)_{ult}}{p_a} = 1/b = 9.139$

$R_f = 0.921$

assumed values in calculation

$a = 0.0248$ from eq. (19)

$b = 0.1129$ » eq. (20)

$E_{ur} = 1/a = 4028$ » eq. (19)

$\frac{(\sigma_1 - \sigma_3)_{ult}}{p_a} = 1/b = 8.861$ » eq. (20)

$R_f = 0.94$ assumed constant

Axial and volumetric strains (eq. 1):

from data of table 1

$A = 120.47$

$B = 1.98$

$r = 0.9755$ (correlation coeff.)

from data of table 1 and eq. (7)

$\nu_i = \nu = 0.045$

from data of tab. 1 and eqs. (14a,b)

$A_3 = 0.001039$ $B_3 = 0.7808$

$A_4 = 0.000136$ $B_4 = 0.6990$

assumed values in calculation (figg. 3a,b)

$A = 126.85$ from eq. (24)

$B = 1.91$

Table 2

CALCULATION OF THE COMPONENTS OF STRAIN IN DRAINED TEST WITH $[\sigma_3/p_a] = 2 =$ const.

CALCOLO DELLE COMPONENTI DI DEFORMAZIONE IN PROVA DRENATA CON $[\sigma_3/p_a] = 2 =$ cost.

deviatoric stresses	total strains			elastic strains		plastic collapse strains					plastic expansive strains	
$(\sigma_1-\sigma_3)/p_a$	$\varepsilon_1 \cdot 10^{+5}$	$\varepsilon_v \cdot 10^{+4}$	$\varepsilon_3 \cdot 10^{+4}$	$\varepsilon^e_1 \cdot 10^{+4}$	$\varepsilon^e_3 \cdot 10^{+5}$	$\Delta\lambda_c \cdot 10^{+4}$	$\Delta\varepsilon^c_1 \cdot 10^{+4}$	$\varepsilon^c_1 \cdot 10^{+3}$	$\Delta\varepsilon^c_3 \cdot 10^{+5}$	$\varepsilon^c_3 \cdot 10^{+4}$	$\varepsilon^p_3 \cdot 10^{+3}$	$\varepsilon^p_1 \cdot 10^{+4}$
0.1	2.51	0.249	−0.000797	0.248	0.112	0.712	0.299	0.0299	2.85	0.285	−0.0297	−0.296
0.5	13.2	1.27	−0.217	1.24	0.559	2.88	1.44	0.174	11.5	1.44	−0.151	−1.66
1.0	28.0	2.61	−0.959	2.48	1.12	3.56	2.13	0.387	14.2	2.86	−0.307	−3.56
1.5	44.8	4.00	−0.241	3.72	1.68	3.40	2.38	0.625	13.6	4.22	−0.463	−5.49
2.0	64.1	5.45	−4.482	4.96	2.23	3.18	2.54	0.879	12.7	5.49	−0.620	−7.35
2.5	86.5	6.94	−0.854	6.21	2.79	2.95	2.65	1.14	11.8	6.67	−0.780	−9.01
3.0	113	8.45	−1.41	7.45	3.45	2.72	2.72	1.42	10.9	7.76	−0.950	−10.4
3.5	144	9.94	−2.21	8.69	3.91	2.50	2.75	1.69	10.0	8.75	−1.14	−11.2
4.0	181	11.3	−3.38	9.93	4.47	2.30	2.76	1.97	9.20	9.67	−1.35	−11.5
4.5	227	12.5	−5.07	11.2	5.03	2.12	2.75	2.24	8.48	10.05	−1.61	−10.9
5.0	285	13.4	−7.56	12.4	5.59	1.96	2.74	2.52	7.83	11.3	−1.94	−9.09
5.5	360	13.4	−11.3	13.7	6.14	1.81	2.72	2.79	7.24	12.0	−2.39	−5.53
6.0	461	12.1	−17.0	14.9	6.70	1.68	2.69	3.06	6.72	12.7	−3.04	−0.673
6.5	606	7.49	−20.3	16.1	7.26	1.56	2.66	3.32	6.25	13.3	−4.04	11.2
7.0	828	−2.01	−42.4	17.4	7.82	1.46	2.62	3.59	5.83	13.9	−5.71	29.5
7.5	1210	−25.7	−73.5	18.6	8.38	1.36	2.59	3.84	5.45	14.5	−8.88	64.2
8.0	2040	−90.7	−148	19.9	8.94	1.28	2.56	4.10	5.11	15.0	−16.3	144
8.5	5190	−382	−450	21.1	9.50	1.20	2.52	4.35	4.80	15.4	−46.7	454

REFERENCES

CHAMBOSSE (1976) - *Stoffansatz fur den Sand unter Verformungsbedingungen im Standard-Trixailversuch Dissertation.* TH Dissertation TH Darmstadt (Dr-Thesis).

DUNCAN J. M., CHANG C. Y. (1970) - *Non linear analysis of stress and strain in soils.* J. of Soil Mech. and Found. Div., Proc. ASCE, N. SM5, pp. 1629-1653.

KONDNER R. L. (1963) - *Hyperbolic stress-strain response: cohesive soils.* J. of Soil Mech. and Found. Div., Proc. ASCE, N. SM1, pp. 115-143.

KONDNER R. L., ZELASKO J. S. (1963) - *Void ratio effects on the hyperbolic stress-strain response of a sand.* ASTM STP N. 361, Ottawa, pp. 250-257.

KULHAWY F. H., DUNCAN J. M. (1972) - *Stresses and movements in Oroville dam.* J. of Soil Mech. and Found. Div., Proc. ASCE, N. SM7, pp. 653-665.

LADE P. V. (1977) - *Elasto-plastic stress strain theory for cohesionless soil with curved yield surface.* Int. J. Solids Struct., vol. 13, pp. 1019-1035.

LADE P. V., DUNCAN J. M. (1973) - *Cubical triaxial tests on cohesionless soil.* J. of Soil Mech. and Found. Div., Proc. ASCE, N. SM10, pp. 793-812.

VANNUCCHI G. (1980) - *Sul comportamento elastico anisotropo di sabbie monogranulari.* UFIST 02/80. Note e Pubblicazioni di Ingegneria Strutturale.

SOMMARIO

Confronto ed uso congiunto di modelli costitutivi diversi per sabbie

Il modello elasto plastico con superfici di plasticizzazione curve per terreni granulari [LADE, 1977] è in grado di descrivere processi di carico complessi, anche successivi alla rottura, con una analisi di tipo incrementale ed ha il grande pregio di poter essere quantitativamente definito attraverso i risultati di prove di compressione isotropa e triassiale standard. Tuttavia i valori direttamente misurati in corso di prove ripetute sono sempre soggetti ad un certo grado di dispersione, sia per le inevitabili differenze nelle caratteristiche geotecniche dei diversi campioni, sia per la limitata sensibilità degli strumenti di misura, sia per errori accidentali compiuti dallo sperimentatore nelle varie fasi di prova. Pertanto se, come si verifica per il modello di Lade, le quantità da valutare sono il risultato di una elaborazione numerica di dati sperimentali di diversa accuratezza e soprattutto se risultano da differenze fra quantità di diverso ordine di grandezza, il risultato può essere poco affidabile anche se ottenuto in modo formalmente corretto.

Nel modello di LADE [1977] le deformazioni totali (volumetriche, assiali, radiali) sono suddivise in tre componenti: elastica, plastica di collasso, plastica espansiva:

— La componente elastica può essere calcolata applicando la legge di Hooke ed utilizzando il modulo di elasticità E_{ur} definito dalla (19).

— Durante una prova di compressione idrostatica, nell'ipotesi di comportamento isotropo, la funzione potenziale plastico g_c coincide con la funzione di plasticizzazione f_c. La componente di deformazione plastica espansiva è nulla. Sottraendo alla deformazione totale misurata la componente elastica calcolata con la legge di Hooke si determina la componente plastica di collasso.

— La legge di incrudimento, determinata sperimentalmente con prova di compressione idrostatica, consente di valutare separatamente gli incrementi delle due componenti di deformazione plastica in prova triassiale drenata.

Nel presente lavoro si propone di utilizzare modelli ausiliari come filtri dei dati sperimentali allo scopo di ridurre i citati effetti negativi impliciti nell'analisi incrementale. In particolare sono stati utilizzati:

— Una relazione sperimentale fra deformazioni volumetriche e pressione di cella in prova di compressione isotropa drenata (eq. 8) [VANNUCCHI, 1980].

— Il modello iperbolico elastico non lineare [DUNCAN e CHANG, 1970] per descrivere la curva tensioni-deformazioni totali fino quasi alla rottura con pochi parametri di facile determinazione e di significato fisico immediato (eq. 16).

— Relazioni sperimentali fra deformazioni volumetriche e assiali in prova di compressione triassiale drenata (eqs. 1 e 2) (Figg. 1 e 2).

— Le deformazioni totali assiali sono calcolate utilizzando la legge iperbolica (18), ove **a** è l'inverso del modulo di scarico e ricarico E_{ur} (eq. 19) e **b** è valutato con il criterio di rottura di Lade (16a) che tiene conto della diminuzione dell'angolo di attrito al crescere della pressione di (eq. 20).

— Le deformazioni totali volumetriche e radiali sono rispettivamente calcolate con la (1) e la (3). I coefficienti A, B, D sono funzioni sperimentali della pressione di consolidazione (24) e (25).

— Le componenti elastiche sono calcolate con la legge di Hooke (10), utilizzando il modulo di elasticità (19) ed il coefficiente di Poisson (7).

— Gli incrementi di deformazione plastica di collasso sono calcolati con la legge di flusso (21) utilizzando la legge di incrudimento (14). L'integrazione delle (21) è eseguita con procedimento numerico.

— Le componenti plastiche espansive sono calcolate per differenza con le (23).

Con tale procedimento si perviene ad una serie di espressioni analitiche che consentono di determinare separatamente le componenti di deformazione (Figg. 4, 5, 6) e le grandezze che caratterizzano il modello di Lade (Figg. 7, 8, 9). Alcune di esse (eq. 25) possono essere confrontate con le corrispondenti espressioni empiriche proposte da Lade (eq. 26) e si verifica un buon accordo nel campo di maggiore rappresentatività dei modelli filtro.

La verifica sperimentale del metodo proposto è stata condotta sulla base dei risultati di 18 prove triassiali standard e di 2 prove di compressione isotropa eseguite su sabbia fine uniforme proveniente da Torre del Lago Puccini (Lucca).

In appendice è riportato un esempio numerico di calcolo.